

Coupled Effects of Ionic Strength, Particle Size, and Flow Velocity on Transport and Deposition of Suspended Particles in Saturated Porous Media

Lyacine Bennacer^{1,2} · Nasre-Dine Ahfir³ ·
Abdellah Alem³ · HuaQing Wang³

Received: 3 November 2016 / Accepted: 27 March 2017 / Published online: 3 April 2017
© Springer Science+Business Media Dordrecht 2017

Abstract In this study, the coupled effect of ionic strength, particle size, and flow velocity on transport and deposition of suspended particles (SP) in saturated sand was undertaken. Three polydisperse SP populations (silt particles with the median of 3.5, 9.5 and 18.3 μm) were investigated using a pulse injection technique. High ionic strengths were used and vary from 0 to 600 mM (NaCl). Two high velocities were tested: 0.15 and 0.30 cm/s. Suspended particles recovery and deposition kinetics were strongly dependent on the solution chemistry, the hydrodynamics, and the suspended particles size, with greater deposition occurring for increasing ionic strength, lower flow velocity, and larger ratios of the median diameter of the SP to the median sand grain diameter. A shift between the extended Derjaguin–Landau–Verwey–Overbeek theory prediction (the particles and sand grain surfaces are considered chemically and topographically homogeneous) and the experimental results for certain ionic strength was observed. So, as reported in recent literature, effects of surface heterogeneities should be considered. The residence time of the non-captured particles is dependent on ionic strength and hydrodynamic. A relationship between the deposition kinetics, particle and grain sizes, flow velocity, and ionic strength is proposed.

Keywords Porous media · Suspended particles size · Physicochemical interaction · Hydrodynamic · Deposition

List of symbols

A Hamaker constant
 a A parameter which depends on the flow velocity (in $a\sqrt{IS}$)

✉ Nasre-Dine Ahfir
ahfir@univ-lehavre.fr

¹ Adrar University, Route Nationale No. 6, 01000 Adrar, Algeria

² Research Laboratory of Applied Hydraulics and Environment, Bejaia University, 06000 Bejaia, Algeria

³ Normandie Univ, UNIHAVRE, UMR 6294 CNRS, LOMC, 76600 Le Havre, France

BTCs	Breakthrough curves
C	DT/SP concentration in solution
C_0	Initial concentration
C_R	Relative concentration
d_{50}	Median diameter
DLVO	Derjaguin–Landau–Verwey–Overbeek
D_L	Longitudinal dispersion coefficient
DT	Dissolved tracer
d_g	Sand grain diameter
d_p	Particles diameter
F_A	Adhesion force
F_{A1}	Adhesive force in the primary minimum
F_{A2}	Adhesion force in the second minimum
F_D	Hydrodynamic drag force
F_G	Gravity force
F_R	Repulsive force
g	Acceleration of gravity
IS	Ionic strength
K	Hydraulic conductivity
k_0	Initial permeability
k_B	Boltzmann constant
K_{dep}	Deposition kinetics coefficient
K_{dep0}	Straining coefficient (value of K_{dep} when IS = 0 mM)
L	Column length
l	Pore diameter
m	Mass of DT/SP injected, equals $V_{inj}C_0$
n	A constant (in $K_{dep0} = \alpha(dp/dg)^n$)
NV_p	Number of pore volumes
Q	Volumetric flow rate
R	Recovery rate
Re	Reynolds number
S	Cross-sectional area
SP	Suspended particles
T	Temperature
t	Time
t_c	Residence time
t_{DT}	Residence time of DT
t_{SP}	Residence time of SP
t_r	Retardation factor, equals t_{SP}/t_{DT}
U	Darcy's velocity
U_p	Fluid velocity at the centre of the solid particle
u	Average pore velocity
V_{inj}	Injected volume
V_p	Pore volume of the porous medium
x	Travel distance (column length)

Greek symbols

α A constant (in $K_{dep0} = \alpha(dp/dg)^n$)

δ	Separation distance between the particle and grain surface
δ_{\max}	Separation distance between particle and grain surface of the energy barriers
δ_{\min}	Separation distance between particle and grain surface of the primary/secondary minimum
λ	Filter coefficient
ϵ_0	Dielectric permittivity
ϵ_r	Relative dielectric permittivity
Φ	Total interaction energy
Φ_{BORN}	Born repulsion interaction energy
Φ_{EDL}	Repulsive electrostatic double-layer interaction energy
Φ_{VDW}	Van der Waals attractive interaction energy
$\Phi_{\min 1}$	Primary minimum
$\Phi_{\min 2}$	Secondary minimum
Φ_{\max}	Energy barrier
γ	A constant (in $K_{\text{dep}} = K_{\text{dep}0} + \gamma U \sqrt{IS}$)
κ_d	Debye length
θ	Characteristic constant of the porous medium
ρ	Specific mass of water
ρ_p	Specific mass of particles
μ	Fluid viscosity
ω	Porosity
ξ_g	Zeta potentials of the sand grains
ξ_p	Zeta potentials of the particles
σ_p	Collision diameter

1 Introduction

The presence of solid particles in soils can facilitate or hinder the transport of contaminants (virus, bacteria, pesticides, metals) to aquifers (McDowell-Boyer et al. 1986; McCarthy and Zachara 1989; Kretzschmar et al. 1997; Sen and Khilar 2006; Gao et al. 2011). Contaminants attached to mobile particles can migrate more rapidly. They can be transported over long distances and can also pose a potential risk for human health and for groundwater resources (Chen et al. 2005). In recent decades, the transport, attachment and detachment of colloidal particles and of micro-organisms in porous media have been largely examined (McDowell-Boyer et al. 1986; Corapcioglu and Jiang 1993; Song and Elimelech 1993; Sayers et al. 1994; Ryan and Elimelech 1996; Shen et al. 2012). However, little research has been done on suspended particles ($> 1 \mu\text{m}$), which can substantially alter soil permeability (internal erosion and clogging) or can become a pollutants vector. Due to their large size and to the relatively less important surface area compared to colloids, their transport has only recently attracted considerable attention (Gohr Pinheiro et al. 1999; Wang et al. 2000; Benamar et al. 2005; Ahfir et al. 2007; Alem et al. 2013; Bennacer et al. 2013; Chen and Bai 2015).

Particles transport mechanisms depend on the hydrodynamic conditions, sedimentation, interception, straining (Herzig et al. 1970; Yao et al. 1971) and particle-particle or particle-collector physicochemical interactions (Tufenkji and Elimelech 2004). These mechanisms are controlled by several factors such as particle size and density (Herzig et al. 1970; Frey et al. 1999; Bennacer et al. 2013; Chrysikopoulos and Katzoyrakis 2015), porous medium structure,

flow velocity (Ahfir et al. 2009) and chemical solution (ionic strength, pH) (Bradford et al. 2007; Shen et al. 2008; Kim et al. 2009; Mesticou et al. 2016).

For larger particles ($>10\ \mu\text{m}$), hydrodynamic, gravity, and inertia effects are more dominant, unlike fine particles, which are essentially subject to physicochemical forces such as electrical double-layer force, Van der Waals attraction forces and Brownian diffusion, which depend in turn on the pH and the ionic strength (Frey et al. 1999; Gohr Pinheiro et al. 1999). Typically, deposited colloidal particles increase with salt concentration in the fluid, and retention reaches a maximal value when this concentration exceeds a certain critical salinity threshold (Khilar and Fogler 1984; Sen and Khilar 2006). The ionic strength effects change with the environment chemical composition and promote the ionic exchanges between water and the porous medium, and according to its intensity, it promotes or not the retention of particles (Grolimund et al. 2001).

Saltwater intrusion into freshwater aquifers, which is most often caused by groundwater pumping from coastal wells, augments salinity (Kaplan and Muñoz-Carpena 2014; Al-Naeem 2014). In this way, groundwater on coastal sides gets invaded by sea waters (Magal et al. 2011). Thus, in certain cases, pumped water is not safe for human consumption. The results presented by Al-Naeem (2014) showed that due to excess pumping in Saq aquifer (Saudi Arabia), total water salinity increased from 950 to 1180 ppm in the unconfined zone and from 600 to 700 ppm in the confined zone.

Since the 1990s, a certain number of studies have shown that brine composition and ionic strength can have an influence on oil recovery (Jadhunandan and Morrow 1995; Tang and Morrow 1999; Li 2011); thereby the low-salinity waterflooding to become an enhanced oil recovery (EOR) method. In the experimental study presented by Cissokho et al. (2009), high- (50 g/L), low- (1 g/L), and very low- (0.1 g/L) salinity brines have been investigated to evaluate the role of microparticles on the low-salinity process in EOR. They observed fine particles migration together with a drastic permeability reduction during one phase low-salinity injection in case of clayey consolidated sandstone porous media. Also, they observed that low-salinity waterflooding increased oil recovery and the process was accompanied by pH increase of the effluent water.

In spite of the number of studies devoted to these area of research, the combined effect of particle size and ionic strength on transport of particles in porous media remains understudied, and much work remains to be explored. Furthermore, very few studies were conducted on high ionic strength close to sea water salinity (Magal et al. 2011), in which particle transport behaviour in soils of high salinity is not well known. The importance of solution chemistry in porous media has been largely examined on colloidal particles that display adequate surface properties (Grolimund et al. 1996; Tripathy 2010; Tosco et al. 2012; Bradford and Torkzaban 2015; Torkzaban et al. 2015), but less research has been devoted to the role of ionic strength in the larger soil particles retention process in porous media. The ionic strengths of the solutions that were used in previous work on colloid transport were usually less than 300 mM (Tufenkji and Elimelech 2005; Johnson et al. 2007; Bradford et al. 2007), and in these studies single solutions with mono-valent salt (NaCl) dominate. A few studies examined solutions with bi-valence salt (Grolimund et al. 2001; Kretzschmar et al. 1997). Magal et al. (2011) and Grolimund et al. (2001) are among the studies which investigated the impact of hyper-saline solutions on colloid transfer. Grolimund et al. (2001) studied solutions of NaCl with ionic strengths ranging between 10 and 1000 mM. In their investigation Magal et al. (2011) studied a wide range of ionic strengths, up to that of Dead Sea brines (containing a variety of salts where the main ones are: Na, K, Ca, Cl, Mg, Sr, SO_4 , Br) with an ionic strength of 8.5 M.

We propose in this paper, a laboratory column experimental study to examine particle transport and deposition, at high flow velocities, in a saturated porous medium by focusing

on the coupled role of suspended particle sizes and of ionic strength using an electrolyte (NaCl) and silt particles of polydisperse distribution. An analytical solution of the convection–dispersion equation with a first-order deposition kinetics was used to determine transport hydrodispersive parameters. The effects of the ionic strength, the flow velocity, and the particle sizes on suspended particles deposition kinetics are discussed.

2 Materials and Methods

2.1 Materials

In order to better understand the transport and deposition behaviour of suspended particles (SP) in saturated porous media, an experimental study dealing with the influence of the SP size, the flow velocity, and the water ionic strength (IS) was undertaken. The experimental system was similar to that used by [Bennacer et al. \(2013\)](#). It consisted of a Plexiglas column of 32 cm length with 4 cm inner diameter and equipped with four pressure sensors [Measurement Specialities (France)] for measuring the pressure variation along the column. The column is fed by a reservoir using a Cole-Parmer Masterflex peristaltic pump with flow rate control. A 5-mL syringe is used to perform pulse injections. The porous medium that filled the column during the experiments consisted of sand collected from Adrar region (Algeria). The grain-size distribution of the sieved sand ranged from 1000 to 1250 μm . Its bulk density and specific density was, respectively, 1.67 and 2.79 g cm^{-3} . The porosity of the porous medium was 0.40 (± 0.01). The water average hydraulic conductivity value of the sand was $K = 5.5 \times 10^{-3} \text{ ms}^{-1}$. To remove all organic matter and fine particles attached to the sand grains, the sand was chemically treated according to a procedure that included a series of acid and base washing as presented by [Ahfir et al. \(2016\)](#). After repeated washing with deionized water, the sand was soaked within nitric acid at a concentration of 0.01 M for 24 h, followed by rinsing with deionized water. After that it was soaked in NaOH (concentration of 0.1 M) for 6 h. Finally, the sand was washed with deionized water until the electrical conductivity of the rinse water was less than 1 $\mu\text{S/cm}$. The sand was then dried for 24 h in an oven at 105 °C.

In order to obtain a homogeneously packed porous medium, the column was partially filled with saline water (the same salinity as in the injection test). Subsequent layers (thickness $\approx 5 \text{ cm}$) were poured into the column, and each layer was packed by vibrating the column ensuring good compaction. To achieve the chemical equilibrium of the saturated porous medium, the column was subjected to continuous flow (0.05 cm/s) during 24 h with the same saline water as for injection test. Then, before SP injection, the porous medium was subjected to the saline water flow, under the velocity to be experimented, during 5 pore volumes. Equilibrium was reached when the pH and the electrical conductivity in the effluent solution were identical to those of the influent solution.

The injected SP consisted of silt collected from Adrar region surface formations. Three populations were selected. According to the particle size distribution curves (Fig. 1) that were acquired using a Coulter Multisizer particle counter (Coulter Electronics) in deionized water (IS = 0 mM NaCl), the size distribution of the first population is ranging from 2 to 8 μm with a median diameter of 3.5 μm (noted SP_3.5 μm). The second population is ranging from 4 to 14 μm with a median diameter of 9.5 μm (noted SP_9.5 μm). The third population is ranging from 10 to 22 μm with a median diameter of 18.3 μm (noted SP_18.3 μm).

To assess the stability of the SP used in the column experiment with respect to coagulation, an experiment was conducted in solution having the same chemical composition as the

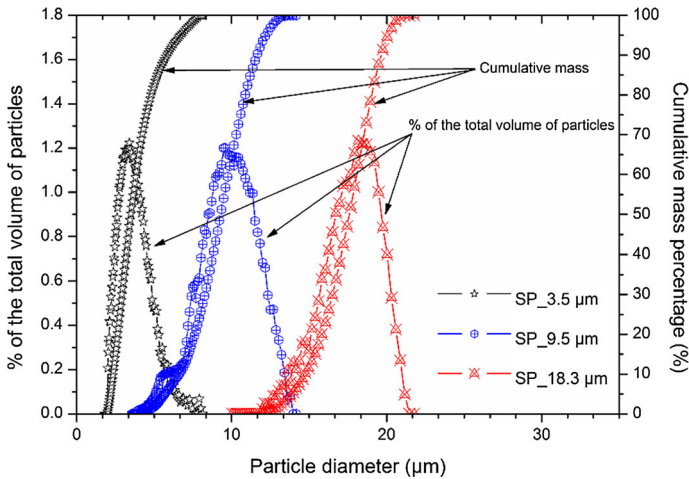


Fig. 1 Particle size distribution of the injected suspended particles

solution used during the corresponding column experiment. Suspensions of 3 g/L SP concentration were prepared in 20-mL beaker of 0, 100, 300, and 600 mM solution. Next, samples of 1 mL were taken periodically (0, 15, 30, 60, 120, and 1440 min) from the solution in order to determine the extent of SP coagulation over time in the beaker by microgranulometric analysis using Coulter Multisizer particle counter. Notice that, before SP sampling in each prepared SP solution, the beaker was slightly agitated during 30 s (60 revolutions/min) to re-suspend the settled SP prior to microgranulometric analysis. The obtained results showed that whatever the IS of the SP solution and the exposition time, there was no variation of the SP diameter. Hence, it was concluded that SP coagulation mechanism is negligible in the present study.

The water used for saturating the medium-filled column and the particles suspension has been prepared at different ionic strength (IS) ranging from 0 to 600 mM, and a pH = 6.5 (± 0.1). The IS is adjusted using sodium chloride (NaCl). The injected volume is very small [$< 3\%$ pore volume (V_p)] with respect to the porous medium pore volume in order to not disturb the water flow in the column. SP concentration was fixed to $C_0 = 3$ g/L for all experiments. A 100-ppb (0.1 mg/L) solution of fluorescein is used as a dissolved tracer (DT) to compare its transport behaviour with that of the SP. Note that, at moderate and high salinities (< 110 g Cl/L), the fluorescein is conservative (Magal et al. 2008). The detection system of the SP and the DT consists, respectively, of a Kobold Instrument Turbidimeter [measurements are displayed in Nephelometric turbidity units (NTU)] and a Turner Designs 10-AU Fluorometer. The particle concentrations in the effluent were determined with the help of correlations made a priori between SP concentrations in water and NTUs. The Fluorometer (calibrated to the fluorescein concentrations) measures DT concentrations in the effluent.

Two flow velocities were tested: 0.15 and 0.30 cm/s corresponding to Reynolds numbers $Re = 1.86$ and $Re = 3.73$, respectively. The duration of the injected pulse was adjusted to the flow velocity tested.

The zeta potential of the sand grains and the SP was measured using a ZetaCAD and ZetaCompact [CAD instrument (France)], respectively, for different values of ionic strength tested. The description of the method used for the zeta potential measurements of the porous media and the SP was presented by Ahfir et al. (2016). The influence of IS on the zeta

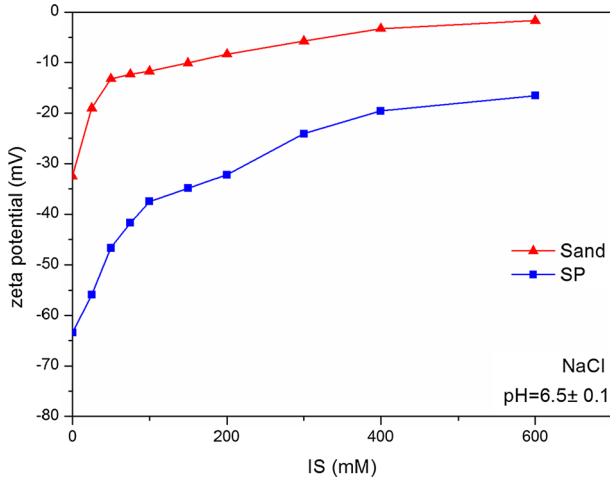


Fig. 2 Zeta potentials of silt particles (SP) and sand grains as a function of ionic strength at unadjusted pH of 6.5 (±0.1)

potentials of the SP and the sand grains is presented in Fig. 2. As shown, the SP and sand grains are negatively charged at the pH of the experiments (6.5 ± 0.1). For all surfaces, the zeta potential becomes less negative with increasing ionic strength due to compression of the electrostatic double layer. These zeta potential values are used later to calculate the extended Derjaguin–Landau–Verwey–Overbeek (DLVO) interaction energies between the SP and the sand grains to elucidate the SP adhesion mechanisms.

2.2 Extended DLVO (XDLVO) Calculations

Particles in an electrolyte solution experience attractive or repulsive interaction energies as they approach the solid–water interface. Theory developed by Derjaguin–Landau–Verwey–Overbeek (DLVO) considers this energy to arise from the superposition of electrostatic and Van der Waals interactions (Derjaguin and Landau 1941; Verwey and Overbeek 1948). Other non-DLVO interactions may occur due to Born repulsion, hydration and hydrophobic forces, and steric interactions (Elimelech et al. 1995). In this study, the total interaction energy Φ for a particle and collector system was considered to be the sum of electrostatic (Φ_{EDL}), van der Waals (Φ_{VDW}), and Born (Φ_{BORN}) repulsion interaction energies:

$$\Phi(\delta) = \Phi_{EDL}(\delta) + \Phi_{VDW}(\delta) + \Phi_{BORN}(\delta) \tag{1}$$

The total interaction energy Φ was calculated by modelling the SP–sand grain system with a sphere–plate interaction. Repulsive electrostatic double-layer interaction energies were calculated using the following expression (Redman et al. 2004):

$$\Phi_{EDL}(\delta) = \epsilon_0 \epsilon_r \cdot \pi \frac{d_p}{2} \left(2\xi_g \xi_p \ln \left(\frac{1 + e^{-\kappa_d \delta}}{1 - e^{-\kappa_d \delta}} \right) + (\xi_g^2 + \xi_p^2) \ln (1 - e^{-2\kappa_d \delta}) \right) \tag{2}$$

where ϵ_0 is the dielectric permittivity in a vacuum (8.854×10^{-12} F/m), ϵ_r is the relative dielectric permittivity of water (equal to 78.4 for water at 20°C), δ is the separation distance between the SP and sand grain surface, d_p is the SP diameter, and κ_d is the Debye length (κ_d^{-1} is the characteristic thickness of the diffuse layer of charge). For water at 20°C, κ_d^{-1}

equals to 3×10^{-10} (IS)^{-0.5} m (Frey et al. 1999), where IS in moles per litre. ξ_p and ξ_g are, respectively, the zeta potentials of the SP and sand grains.

The Van der Waals attractive interaction energy was calculated as follows (Bhattacharjee and Elimelech 1997):

$$\Phi_{VDW}(\delta) = -\frac{A}{12} \left(\frac{d_p}{\delta} + \frac{d_p}{(d_p + \delta)} + 2 \ln \left(\frac{\delta}{d_p + \delta} \right) \right) \tag{3}$$

where A is the Hamaker constant of the interacting media (SP-water-sand). A value of 10^{-20} J was retained for the Hamaker constant (inorganic particles) (Tufenkji and Elimelech 2004).

Born repulsion, Φ_{ORN} , was calculated from (Ruckenstein and Prieve 1976) as:

$$\Phi_{BORN}(\delta) = \frac{A\sigma_p^6}{7560} \left(\frac{4d_p + \delta}{(d_p + \delta)^7} + \frac{3d_p - \delta}{\delta^7} \right) \tag{4}$$

where σ_p is collision diameter and usually is taken as $\sigma_p = 0.5$ nm (Khilar et al. 1990; Ryan and Gschwend 1994; Elimelech et al. 1995).

The XDLVO interaction energy profiles for the SP were calculated using the measured zeta potentials at different IS. The interaction energies are commonly made dimensionless by dividing by the product of the Boltzmann constant ($k_B = 1.38 \times 10^{-23}$ JK⁻¹) and the absolute temperature T (K).

2.3 Forces Evaluation

This section contains details pertaining to drag forces (F_D), adhesive forces (F_A), repulsive forces (F_R), and gravity forces (F_G) calculations.

The drag force F_D operating on a spherical particle of diameter d_p in contact with a plane wall in a laminar flow is expressed as (Goldman et al. 1967; O'Neill 1968):

$$F_D = (1.7005)(3\pi\mu U_p d_p) \tag{5}$$

where μ is the fluid viscosity and U_p is the fluid velocity at the centre of the solid particle. U_p is expressed as (Sharma et al. 1992):

$$U_p = 6 \left(\frac{Q}{S} \right) \left(\frac{d_p}{2l} \right) \left(1 - \frac{d_p}{2l} \right) \tag{6}$$

where Q is the volumetric flow rate, S is the cross-sectional area, and l is the spacing between the two plane walls. To adapt these flow parameters to porous media, $\frac{Q}{S}$ could be approximated as the pore velocity and l as the pore diameter (Ryan and Elimelech 1996). The pore diameter l can be estimated as (Minssieux et al. 1998):

$$l = 2\theta \sqrt{\frac{8k_0}{\omega}} \tag{7}$$

where ω is the porous medium porosity, k_0 is the initial permeability [m²], and θ is a characteristic constant of the porous medium ($\theta = 1.15$ for granular packs).

The adhesive forces F_A were estimated as (Torczaban et al. 2007):

$$F_A = \frac{|\Phi_{\min}|}{\delta_{\min}} \tag{8}$$

where $|\Phi_{\min}|$ is the absolute value of the primary or secondary minima interaction energy and δ_{\min} is the separation distance between the particle and the grain surface.

In this study F_{A1} , F_{A2} refers, respectively, to adhesive force in the primary minimum and adhesive force in the secondary minimum.

The repulsive force F_R is estimated as the ratio of the energy barrier Φ_{\max} value to the separation distance δ_{\max} as:

$$F_R = \frac{\Phi_{\max}}{\delta_{\max}} \quad (9)$$

The gravity force F_G was estimated as (Herzig et al. 1970):

$$F_G = \frac{\pi d_p}{6} (\rho_p - \rho) g \quad (10)$$

where g is the acceleration of gravity, ρ is the specific mass of carrier fluid, and ρ_p is the specific mass of particles.

Particles attachment was only possible on regions of the grain surface where the hydrodynamic drag forces acting on SP adjacent to grain surfaces were less than the adhesive forces and the gravity forces that resist release.

2.4 Identification of the Transport Parameters

In this study, one-dimensional transport experiments (short pulse injection) were conducted in saturated sand column under constant flow velocities. SP concentration breakthrough data obtained at the outlet of the packed columns were analysed by the convection–dispersion equation (CDE) including a term of a first-order deposition kinetics (Kretzschmar et al. 1997; Wang et al. 2000).

$$\frac{\partial C}{\partial t} = D_L \frac{\partial^2 C}{\partial x^2} - u \frac{\partial C}{\partial x} - K_{\text{dep}} C \quad (11)$$

where C is the particle concentration in solution (ML^{-3}), t is the elapsed time (T), x is the travel distance (L), D_L is the longitudinal dispersion coefficient ($\text{L}^2 \text{T}^{-1}$), u is the average velocity of particles (L T^{-1}), and K_{dep} is the SP deposition rate coefficient (T^{-1}). In Eq. 11, SP deposition was assumed to follow first-order kinetics, to be irreversible and particle release is neglected. An implicit assumption of the first-order model is that deposition occurs under clean bed conditions. This assumption is justified at sufficiently low particle concentration (i.e. no blocking or ripening) (Elimelech et al. 1995; Kretzschmar et al. 1997).

For pulse injection condition, the analytical solution for Eq. 11 is given as follows (Wang et al. 2000):

$$C(t, x) = \frac{mx}{Q\sqrt{4\pi D_L t^3}} \exp(-K_{\text{dep}} t) \exp\left(-\frac{(x - ut)^2}{4D_L t}\right) \quad (12)$$

where m is the mass of particles injected (M). Based on the analytical solution (Eq. 12), the regression parabolic method (Wang et al. 2000; Bennacer et al. 2013) is used in order to determine the SP transport parameters (D_L , K_{dep} , and the residence time t_c). Note that, as mentioned in the experimental section, the DT (fluorescein) used in this study is conservative (non-retained and non-reactive) tracer even at high ISs used. Thus, no deposition (adsorption) occurs ($K_{\text{dep}} = 0$ in Eq. 12) for the DT, and only two parameters were determined (D_L and t_c).

Throughout the rest of this article, the discussion of the experimental data is based on the calculations of the involved forces (F_D (Eq. 5), F_A (Eq. 8), F_R (Eq. 9), and F_G (Eq. 10)) and the transport parameters (D_L , t_c , and K_{dep}) (Eq. 12).

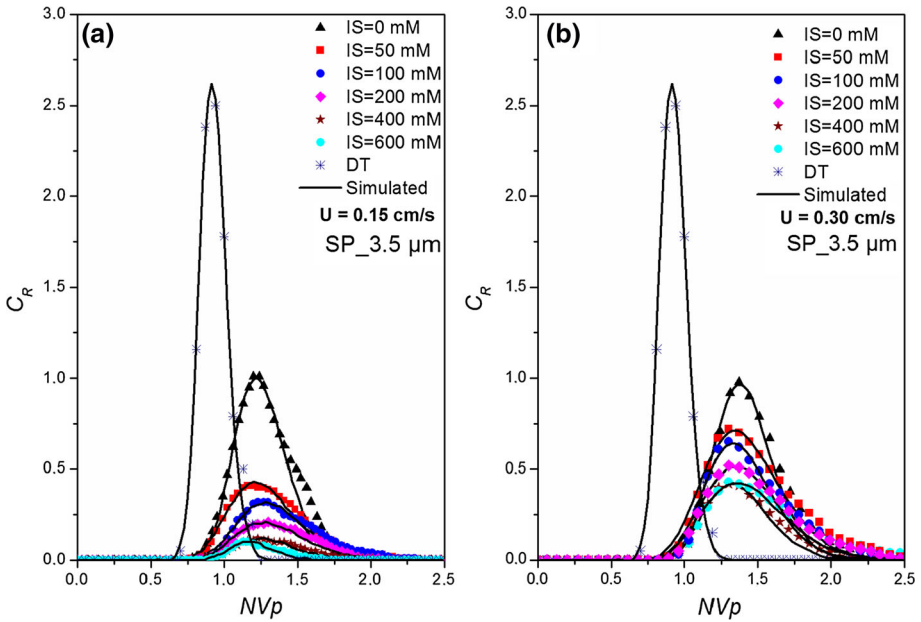


Fig. 3 Experimental and simulated breakthrough curves of the suspended particles (SP_{3.5} μm) and the dissolved tracer (DT) for flow velocities: **a** $U = 0.15$ cm/s and **b** $U = 0.30$ cm/s

3 Results and Discussion

3.1 Transport Behaviour of Particles

Figure 3 presents BTCs of SP_{3.5} μm and the DT for the two flow velocities experienced in this study. Also, it shows comparisons between experimental data and those computed according to the analytical solution (Eq. 12) presented above allowing the determination of the hydrodispersive parameters of the porous medium. The BTCs are represented by the relative concentration C_R versus the number of pore volumes NV_p :

$$C_R = \frac{NV_p C}{V_{inj} C_0} = \frac{\int_0^\infty Q C dt}{V_{inj} C_0} \tag{13}$$

$$NV_p = \frac{Qt}{V_p} \tag{14}$$

where V_{inj} is the solute injected volume (L^3), V_p is the pore volume of the porous medium (L^3), and C_0 is the initial concentration (ML^{-3}).

Figure 3 shows a shift between DT BTCs and SP BTCs indicating that the residence time of the SP in the porous medium was more important than the residence time of the DT as it will be discussed below. For the DT, the recovery rate varies little with the flow velocity and ionic strength; its value is around 100%. Also, whatever the flow velocity, the peak of the SP BTCs decreases with increasing IS. This behaviour will be discussed in this section thereafter.

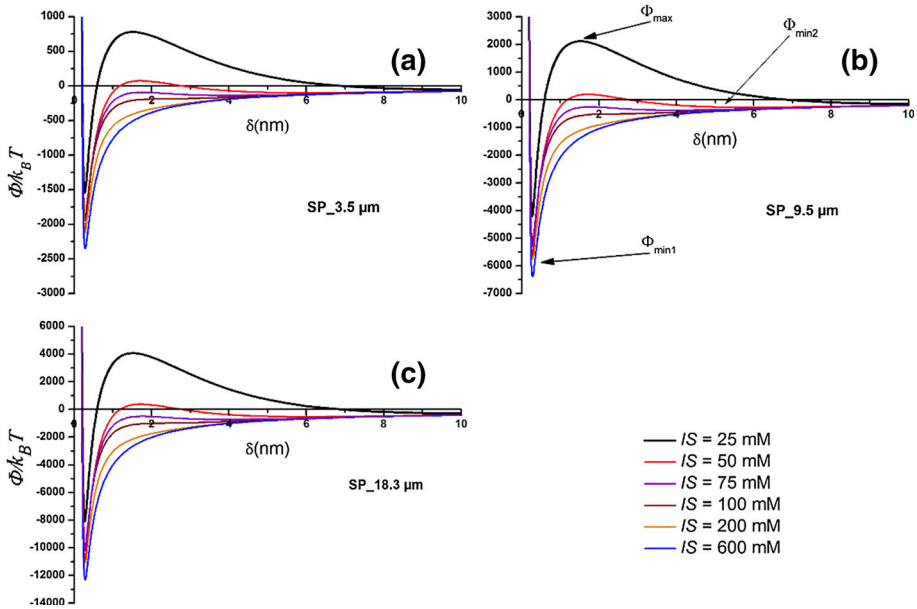


Fig. 4 XDLVO Interaction energies for different ionic strength (IS) values as a function of surface-to-surface separation distance (δ) for different SP population: **a** 3.5 μm , **b** 9.5 μm , and **c** 18.3 μm

Figure 4 presents the evolution of the interaction energies (XDLVO) for different IS values as a function of surface-to-surface separation distance (δ) for the different SP population studied. For clarity, only six out of ten ISs used in this study are presented. For ISs equal to or less than 50 mM, the XDLVO calculations predict the presence of substantial repulsive energy barriers. For the SP_3.5 μm , the energy barriers are ranging from 74.4 $k_B T$ at 50 mM to 781 $k_B T$ at 25 mM, and relatively shallow secondary minimums ($-98.1 k_B T$ at 50 mM to $-54.9 k_B T$ at 25 mM). The depth of the primary minimum $\Phi_{\text{min}1}$ increases with ISs increasing. The magnitude of the interaction energies increases with increasing SP size.

For $IS \leq 50 \text{ mM}$, whatever the flow velocity, the particle sizes, the calculations indicate that the hydrodynamic drag forces, F_D , are negligible compared to the repulsive forces, F_R . To give an idea about the importance of repulsive forces, F_R , to the hydrodynamic drag forces, F_D , the calculations done for a particle of 8 μm when $IS = 50 \text{ mM}$ and for the highest flow velocity $U = 0.30 \text{ cm/s}$ show that $F_R = 23 F_D$.

For the flow velocity $U = 0.15 \text{ cm/s}$, whatever the particle sizes in different SP populations tested (SP_3.5 μm , SP_9.5 μm , and SP_18.3 μm) F_D is negligible compared to $F_{A2} + F_G$ when $IS \leq 50 \text{ mM}$ indicating that the attachment of the SP occurs in the secondary minimum. The same results were obtained for the flow velocity $U = 0.30 \text{ cm/s}$, when the $IS = 50 \text{ mM}$. For the latter flow velocity ($U = 0.30 \text{ cm/s}$) and when $IS = 25 \text{ mM}$, attachment in the secondary minimum occurs for all particle sizes constituting the population SP_3.5 μm . However, for the particle sizes greater than 9 μm , the hydrodynamic forces, F_D , are larger than the sum of adhesion and gravity forces ($F_{A2} + F_G$). In other words, it concerns a part of the particles of the population SP_9.5 μm and the entire population SP_18.3 μm . This result indicates that for $IS = 25 \text{ mM}$ and for particles larger than 9 μm , SP deposition occurs mainly by straining at $U = 0.3 \text{ cm/s}$.

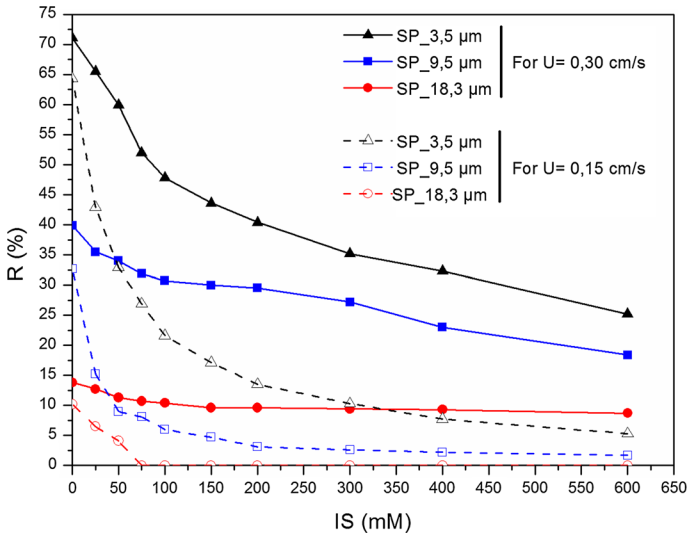


Fig. 5 SP recovery rate (R) as a function of ionic strength (IS). Influence of the particle size and flow velocity (U)

The calculations done for all particle sizes tested in this study for $IS = 0$ mM and whatever the flow velocity tested, show that the dominant mechanism to particles deposition is straining (F_D is very weak compared to F_R and higher than $F_{A2} + F_G$). Notice that, beyond 50 mM there are favourable conditions for SP deposition, and all particles approaching the grain surface beyond 10 nm are attached.

Figure 5 shows the evolution of the particles recovery rate [R (%)] as a function of IS for both flow velocities tested. R (%) is estimated by integrating the experimental BTCs. The recovery rate R (%) decreases with increasing IS as expected for the IS s larger than 50 mM where favourable conditions to SP deposition exist. As discussed above, following the different forces calculations, SP deposition occurs in the secondary minimum except for the particles larger than 9 μ m when $IS = 25$ mM and for $U = 0.30$ cm/s.

For $IS = 0$ mM, unfavourable conditions to SP deposition (whatever the particle sizes in different SP populations tested) were predicted for both flow velocities tested, and SP were captured mainly by straining. However, although the deposition conditions are unfavourable when $IS = 25$ mM and for $U = 0.30$ cm/s, results show that for the population SP_18.3 μ m the SP recovery rate decreases when the IS changes from 0 to 25 mM. A possible explanation of this behaviour is that, in the calculations done in this study, the particles and sand grain surfaces are considered chemically and topographically (roughness) homogeneous. The pore structure and surface roughness induce a shift of the actual interaction potential. Indeed, surface roughness favours deposition in secondary minima (Shen et al. 2012).

For the population SP_18.3 μ m and for $U = 0.15$ cm/s, the particles are totally retained in the porous medium when $IS \geq 75$ mM. This result shows that for larger particles and when the hydrodynamic forces are too low compared to adhesion and gravity forces (for example, when $IS = 75$ mM, $F_{A2} + F_G = 14 F_D$ for a particle of 10 μ m), deposition is inevitable.

From Fig. 5, it arises that at a given IS , a better recovery rate is obtained when the flow velocity is high. As expected, for a given flow velocity and regardless of the IS tested, SP recovery rate decreases as the size of the injected particles increases. These results show the

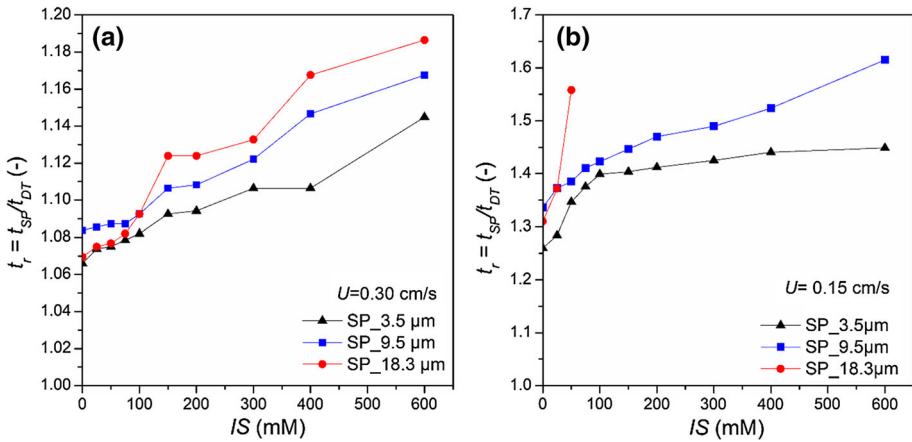


Fig. 6 Retardation factor t_r (ratio of the SP residence time (t_{SP}) to the DT residence time (t_{DT})) as a function of ionic strength (IS): **a** $U = 0.30$ cm/s and **b** $U = 0.15$ cm/s

importance of hydrodynamic forces, which are strongly related to the size of the transported particles.

The breakthrough of the DT occurred earlier than the breakthrough of the SP for all flow velocities and IS tested (Cf. Fig. 3). A retardation factor noted t_r is defined as the ratio t_{SP}/t_{DT} , where t_{SP} and t_{DT} are, respectively, the residence time of the non-captured SP and of the DT in the porous medium. Figure 6 shows the variation of t_r as a function of IS for the two flow velocities tested. For the same SP population, the evolution of the retardation factor t_r is velocity dependent. When $U = 0.30$ cm/s and for unfavourable deposition condition (IS = 0 mM), the values of the retardation factor t_r obtained were between 1.06 and 1.09. For $U = 0.15$ cm/s and for IS = 0 mM, the values of t_r were between 1.25 and 1.35. Also, Figure 6 shows that the retardation factors t_r increase when the size of the transported SP increases.

The retardation factor t_r increases with increasing IS. It reaches 1.19 when the flow velocity was 0.30 cm/s for the largest SP (SP_18.3 μm) tested (Fig. 6a). When the flow velocity used equals 0.15 cm/s, the retardation factor reaches values greater than 1.5 (Fig. 6b). Also, for a given IS, and regardless of the size of the particles transported, when the flow velocity is reduced by half (i.e. when U pass from 0.30 to 0.15 cm/s) the value of t_r increases, on average, by 0.30 (this average value is calculated on the 10 ISs tested).

These results indicate that for a fixed flow velocity, the residence time of the SP increases with increasing IS as the particles pore surfaces become less repulsive. Sefrioui et al. (2013) showed the same behaviour using a numerical simulation of retention and release of colloids in porous media at the pore scale. Finally, these results show that the residence time of the non-captured particles is dependent on IS and hydrodynamic.

3.2 Deposition Kinetics

Kinetics deposition coefficient (K_{dep}) is the parameter which characterizes particles deposition rate by the different mechanisms (sedimentation, straining, interception ...) in the porous medium. K_{dep} is obtained by fitting the experimental SP BTCs according to Eq. 12 using the regression parabolic method (Bennacer et al. 2013). As discussed above (Sect. 3.1), particles are mainly captured by straining when IS = 0 mM (high energy barrier). With IS increasing,

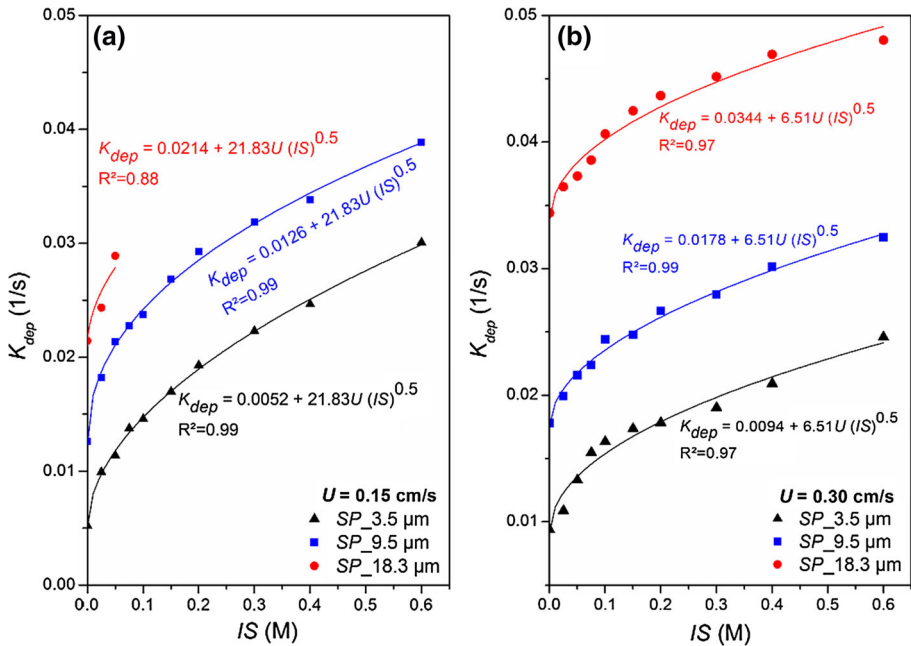


Fig. 7 Deposition kinetics coefficient K_{dep} evolution as a function of the ionic strength (IS) for the different particle size: **a** $U = 0.15 \text{ cm/s}$ and **b** $U = 0.30 \text{ cm/s}$

the particles are subject either to attractive forces in secondary minimum [when $IS < 50 \text{ mM}$ (except for $IS = 25 \text{ mM}$ and for $U = 0.30 \text{ cm/s}$ when SP sizes were larger than $9 \mu\text{m}$)] or in primary minimum ($IS > 75 \text{ mM}$). Gravity effects could not be neglected for large particles and when the particle approaches to the grain surface (for $\delta < 10 \text{ nm}$). In Fig. 7 is presented the deposition kinetics coefficient K_{dep} as a function of IS at $U = 0.15 \text{ cm/s}$ (Fig. 7a) and $U = 0.30 \text{ cm/s}$ (Fig. 7b). Results show that K_{dep} increases with increasing IS. For a constant flow velocity and at given IS, K_{dep} is high when SP sizes are large. Also, K_{dep} decreased with increasing flow velocity, suggesting a mitigating effect of hydrodynamic forces on deposition.

Results show that the kinetics deposition coefficient K_{dep} is proportional to the square root of the IS according to the following relationship:

$$K_{dep} = K_{dep0} + a\sqrt{IS} \tag{15}$$

where K_{dep0} is the value of K_{dep} in pure water ($IS = 0 \text{ mM}$) and represents the kinetics deposition by straining. The term " $a\sqrt{IS}$ " in Eq. (15) quantifies secondary and primary minimum attachment kinetics, with " a " a parameter which depends on the flow velocity.

Equation 15 can be rewritten as follows:

$$K_{dep} = K_{dep0} + \gamma U \sqrt{IS} \tag{16}$$

where an average value of " γ " to be considered is 6.51 when $U = 0.30 \text{ cm/s}$ and 21.83 when $U = 0.15 \text{ cm/s}$ [these values are obtained when IS and U , respectively, are given in terms of moles per litre (M) and m/s].

The SP size effect on deposition kinetics is included in K_{dep0} . K_{dep0} increases with increasing flow velocity. For a given flow velocity and when the IS is zero, K_{dep0} increases with the particle size. This result was expected to the extent that retention of the SP for $IS = 0$

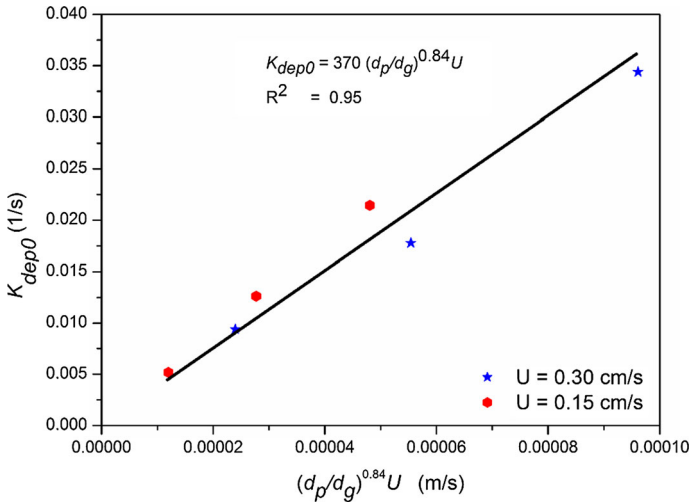


Fig. 8 Simultaneous effects of the flow velocity and the particles sizes (presented by the ratio of d_p/d_g) on the straining coefficient

is dominated by straining. Bradford et al. (2003) proposed a power relationship between the straining coefficient (K_{dep0}) and the ratio d_p/d_g [$K_{dep0} = \alpha(d_p/d_g)^n$]. Other authors (Xu et al. 2006; Porubcan and Xu 2011; Raychoudhury et al. 2014) suggest a linear relationship between the straining coefficient K_{dep0} and d_p/d_g .

In this study, similar relationship to that proposed by Bradford et al. (2003) is considered. Results show that the coefficient α increases linearly with flow velocity ($\alpha = 370U$). Figure 8 summarizes the simultaneous effects of the flow velocity and the ratio of d_p/d_g on the straining coefficient. Thus, the influences of both particle size diameter and flow velocity on SP deposition “by straining” can be described by the following relationship:

$$K_{dep0} = 370 \left(\frac{d_p}{d_g} \right)^{0.84} U \tag{17}$$

This evolution of K_{dep0} (Eq. 17) is similar to that proposed by Foppen et al. (2005) who studied *Escherichia coli* straining in two different sands under several flow velocities.

Combining Eqs. (16) and (17) yields

$$K_{dep} = \left(\alpha \left(\frac{d_p}{d_g} \right)^{0.84} + \gamma \sqrt{IS} \right) U \tag{18}$$

Equation (18) is a global relationship that considers for straining and attachment in the secondary and primary minimum. The latter equation (Eq. 18) is similar to that used in filtration theory where the deposition kinetics coefficient is related to the filter coefficient λ (Tien 1989). In the same vein, Foppen and Schijven (2006) proposed a similar formulation of the kinetics deposition coefficient which takes into account the deposition by straining and by attachment.

4 Conclusion

The work realized in this study aimed at exploring the coupled effects of ionic strength, particle size, and flow velocity on transport and deposition of suspended particles in saturated sand filling a laboratory column. Compared to the majority of the work reported in the literature, this study, high ionic strengths are investigated (from 0 to 600 mM NaCl). To evaluate the suspended particles–sand grain interaction, extended DLVO (XDLVO) theory was used. Suspended particles and sand grain surfaces are considered chemically and topographically homogeneous. Suspended particles recovery and deposition kinetics were strongly dependent on the solution ionic strength, the hydrodynamics, and the suspended particle sizes, with greater deposition occurring for increasing ionic strength, low flow velocity, and larger ratios of the median diameter of the suspended particles to the median sand grain diameter. Among the results highlighted:

- A shift was observed between the XDLVO theory prediction (presence of repulsion barrier and hydrodynamic drag forces larger than adhesive forces in the secondary minimum) and the experimental results for a certain ionic strength ($IS = 25 \text{ mM}$) and when the particle sizes were larger than $9 \mu\text{m}$. A possible explanation of this behaviour is due, as reported in recent literature, to the effects of surface heterogeneities that should be considered.
- For a fixed flow velocity and particle size, the residence time of the non-captured particles increases with increasing ionic strength as the particle/grain surface becomes less repulsive. For a given IS, the retardation of the SP compared to the DT was less important when the flow velocity was high. The residence time of the non-captured particles is dependent on IS and flow velocity.
- A relationship summarizing the simultaneous effects of particle size, flow velocity, and ionic strength on deposition kinetics coefficient is proposed. This relationship considers for straining and attachment mechanisms.

Furthermore, in view of these results, it would be interesting to analyse the experimental data presented in this study using a numerical modelling where the effects of surface heterogeneities on the retention of the particles in the second minimum will be considered even under unfavourable conditions to deposition.

Acknowledgements This work was supported by Région Haute Normandie_R2015-CPER-0054A.

References

- Ahfir, N.-D., Wang, H.Q., Benamar, A., Alem, A., Masséi, N., Dupont, J.-P.: Transport and deposition of suspended particles in saturated porous media hydrodynamic effect. *Hydrol. J.* **15**, 659–668 (2007)
- Ahfir, N.-D., Benamar, A., Alem, A., Wang, H.Q.: Influence of internal structure and medium length on transport and deposition of suspended particles: a laboratory study. *Transp. Porous Media* **76**, 289–307 (2009)
- Ahfir, N.-D., Hammadi, A., Alem, A., Wang, H.Q., Le Bras, G., Ouahbi, T.: Porous media grain size distribution and hydrodynamic forces effects on transport and deposition of suspended particles. *J. Environ. Sci.* (2016). doi:[10.1016/j.jes.2016.01.032](https://doi.org/10.1016/j.jes.2016.01.032)
- Alem, A., Elkawafi, A., Ahfir, N.-D., Wang, H.Q.: Filtration of kaolinite particles in a saturated porous medium: hydrodynamic effects. *Hydrol. J.* **21**, 573–586 (2013)
- Al-Naeem, A.: Effect of excess pumping on groundwater salinity and water level in Hail region of Saudi Arabia. *Res. J. Environ. Toxicol.* **8**(3), 124–135 (2014)

- Benamar, A., Wang, H.-Q., Ahfir, N.-D., Alem, A., Masséi, N., Dupont, J.-P.: Flow velocity effects on the transport and the deposition rate of suspended particles in a saturated porous medium. *C. R. Geosci.* **337**, 497–504 (2005)
- Bennacer, L., Ahfir, N.-D., Bouanani, A., Alem, A., Wang, H.-Q.: Suspended particles transport and deposition in saturated granular porous medium: particle size effects. *Transp. Porous Media* **100**, 377–392 (2013)
- Bhattacharjee, S., Elimelech, M.: Surface element integration: a novel technique for evaluation of DLVO interaction between a particle and a flat plate. *J. Colloid Interface Sci.* **193**, 273–285 (1997)
- Bradford, S.A., Simunek, J., Bettahar, M., Van Genuchten, M.T.-H., Yates, S.R.: Modeling colloid attachment, straining, and exclusion in saturated porous media. *Environ. Sci. Technol.* **37**, 2242–2250 (2003)
- Bradford, S.A., Torkzaban, S., Walker, S.L.: Coupling of physical and chemical mechanisms of colloid straining in saturated porous media. *Water Res.* **41**, 3012–3024 (2007)
- Bradford, S.A., Torkzaban, S.: Determining parameters and mechanisms of colloid retention and release in porous media. *Langmuir* **31**, 12096–12105 (2015)
- Chen, X., Bai, B.: Experimental investigation and modeling of particulate transportation and deposition in vertical and horizontal flows. *Hydrol. J.* **23**, 365–375 (2015)
- Chen, J.C., Elimelech, M., Kim, A.S.: Monte Carlo simulation of colloidal membrane filtration model development with application to characterization of colloid phase transition. *J. Membr. Sci.* **255**, 291–305 (2005)
- Chrysikopoulos, C.V., Katzoarakis, V.E.: Colloid particle size-dependent dispersivity. *Water Resour. Res.* **51**, 4668–4683 (2015). doi:[10.1002/2014WR016094](https://doi.org/10.1002/2014WR016094)
- Cissokho, M., Boussour, S., Cordier, Ph., Bertin, H., Hamon, G.: Low salinity oil recovery on clayey sandstone: experimental study. Paper SCA 2009-05 presented at the 23rd International Symposium of the Society of Core Analysts, Noordwijk, 27–30 September (2009)
- Corapcioglu, M.Y., Jiang, S.: Colloid-facilitated groundwater contaminant transport. *Water Resour. Res.* **29**(7), 2215–2226 (1993)
- Derjaguin, B.V., Landau, L.D.: Theory of the stability of strongly charged lyophobic sols and of the adhesion of strongly charged particles in solutions of electrolytes. *Acta Physicochim. USSR* **14**, 733–762 (1941)
- Elimelech, M., Gregory, J., Jia, X., Williams, R.A.: *Particle Deposition and Aggregation Measurement, Modeling, and Simulation*. Butterworth-Heinemann, Oxford (1995)
- Foppen, J.W.A., Mporokoso, A., Schijven, J.F.: Determining straining of *Escherichia coli* from breakthrough curves. *J. Contam. Hydrol.* **76**, 191–210 (2005)
- Foppen, J.W.A., Schijven, J.F.: Evaluation of data from the literature on the transport and survival of *Escherichia coli* and thermotolerant coliforms in aquifers under saturated conditions. *Water Res.* **40**, 401–426 (2006)
- Frey, J.M., Schmitz, P., Dufreche, J., Gohr Pinheiro, I.: Particle deposition in porous media: analysis of hydrodynamic and weak inertial effects. *Transp. Porous Media* **37**, 25–54 (1999)
- Gao, B., Cao, X., Dong, Y., Luo, Y., Ma, L.Q.: Colloid deposition and release in soils and their association with heavy metals. *Crit. Rev. Environ. Sci. Technol.* **41**(4), 336–372 (2011)
- Gohr Pinheiro, I., Schmitz, P., Houi, D.: Particle capture in porous media when physico-chemical effects dominate. *Chem. Eng. Sci.* **54**, 3801–3813 (1999)
- Goldman, A.J., Cox, R.G., Brenner, H.: Slow viscous motion of a sphere parallel to a plane wall—II Couette flow. *Chem. Eng. Sci.* **22**(4), 653–660 (1967)
- Grolimund, D., Borkovec, M., Barmettler, K., Sticher, H.: Colloid-facilitated transport of strongly sorbing contaminants in natural porous media: a laboratory column study. *Environ. Sci. Technol.* **30**, 3118–3123 (1996)
- Grolimund, D., Barmettler, K., Borkovec, M.: Release and transport of colloidal particles in natural porous media: 2. Experimental results and effects of ligands. *Water Resour. Res.* **37**(3), 571–582 (2001)
- Herzig, J.P., Leclerc, D.M., Le Goff, P.: Flow of suspension through porous media—application to deep bed filtration. *Ind. Eng. Chem.* **62**, 8–35 (1970)
- Jadhunandan, P.P., Morrow, N.R.: Effect of wettability on waterflooding recovery for crude oil/brine/rock systems. *SPE Reserv. Eng.* **10**(1), 40–46 (1995)
- Johnson, W.P., Li, X., Assemi, S.: Deposition and re-entrainment dynamics of microbes and non-biological colloids during non-perturbed transport in porous media in the presence of an energy barrier to deposition. *Adv. Water Resour.* **30**, 1432–1454 (2007)
- Kaplan, D.A., Muñoz-Carpena, R.: Groundwater salinity in a floodplain forest impacted by saltwater intrusion. *J. Contam. Hydrol.* **169**, 19–36 (2014)
- Khilar, K.C., Fogler, H.S.: The existence of a critical salt concentration for particle release. *J. Colloid Interface Sci.* **101**(1), 214–224 (1984)
- Khilar, K.C., Vaidya, R.N., Fogler, H.S.: Colloidally-induced fines release in porous media. *J. Pet. Sci. Eng.* **4**, 213–221 (1990)

- Kim, H.N., Bradford, S.A., Walker, S.L.: *Escherichia coli* O157 H7 transport in saturated porous media: role of solution chemistry and surface macromolecules. *Environ. Sci. Technol.* **43**, 4340–4347 (2009)
- Kretzschmar, R., Barmettler, K., Grolimund, D., Yan, Y.D., Borkovec, M., Sticher, H.: Experimental determination of colloid deposition rates and collision efficiencies in natural porous media. *Water Resour. Res.* **33**(5), 1129–1137 (1997)
- Li, Y.: Oil recovery by low salinity water injection into a reservoir: a new study of tertiary oil recovery mechanism. *Transp. Porous Media.* **90**, 333–362 (2011)
- Magal, E., Weisbrod, N., Yakirevich, A., Yechieli, Y.: The use of fluorescent dyes as tracers in highly saline groundwater. *J. Hydrol.* **358**, 124–133 (2008)
- Magal, E., Weisbrod, N., Yechieli, Y., Walker, S.L., Yakirevich, A.: Colloid transport in porous media: impact of hyper-saline solutions. *Water Res.* **45**, 3521–3532 (2011)
- McCarthy, J.F., Zachara, J.M.: Subsurface transport of contaminants. *Environ. Sci. Technol.* **23**, 496–502 (1989)
- McDowell-Boyer, L.M., Hunt, J.R., Sitar, N.: Particle transport through porous media. *Water Resour. Res.* **22**(13), 1901–1921 (1986)
- Mesticou, Z., Kacem, M., Dubujet, P.: Coupling effects of flow velocity and ionic strength on the clogging of a saturated porous medium. *Transp. Porous Media* **112**, 265–282 (2016)
- Minssieux, L., Nabzar, L., Chauveteau, G., Longeron, D., Bensalem, R.: Permeability damage due to asphaltene deposition: experimental and modeling aspects. *Revue Française de l'institut du Pétrole.* **53**(3), 313–327 (1998)
- O'Neill, M.E.: A sphere in contact with a plane wall in slow linear shear flow. *Chem. Eng. Sci.* **23**, 1293–1298 (1968)
- Porubcan, A.A., Xu, S.: Colloid straining within saturated heterogeneous porous media. *Water Res.* **45**, 1796–1806 (2011)
- Raychoudhury, T., Tufenkji, N., Ghoshal, S.: Straining of polyelectrolyte-stabilized nanoscale zero valent iron particles during transport through granular porous media. *Water Res.* **50**, 80–89 (2014)
- Ryan, J.N., Gschwend, P.M.: Effects of ionic strength and flow rate on colloid release: relating kinetics to intersurface potential energy. *J. Colloid Interface Sci.* **164**, 21–34 (1994)
- Ryan, J.N., Elimelech, M.: Colloid mobilisation and transport in groundwater. *Colloids Surf. A* **107**, 1–56 (1996)
- Redman, R.A., Walker, S.L., Elimelech, M.: Bacterial adhesion and transport in porous media role of the secondary energy minimum. *Environ. Sci. Technol.* **38**, 1777–1785 (2004)
- Ruckenstein, E., Prieve, D.C.: Adsorption and desorption of particles and their chromatographic separation. *AIChE J.* **22**, 276–285 (1976)
- Saiers, J.E., Hornberger, G.M., Liang, L.: First- and second-order kinetics approaches for modeling the transport of colloidal particles in porous media. *Water Resour. Res.* **30**(9), 2499–2506 (1994)
- Sefrioui, N., Ahmadi, A., Omari, A., Bertin, H.: Numerical simulation of retention and release of colloids in porous media at the pore scale. *Colloids Surf. A* **427**, 33–40 (2013)
- Sen, T.K., Khilar, K.C.: Review on subsurface colloids and colloid-associated contaminant transport in saturated porous media. *Adv. Colloid Interface Sci.* **119**, 71–96 (2006)
- Sharma, M.M., Chamoun, H., Sarma, D.S.H.S.R., Schechter, R.S.: Factors controlling the hydrodynamic detachment of particles from surfaces. *J. Colloid Interface Sci.* **149**(1), 121–134 (1992)
- Shen, C., Huang, Y., Li, B., Jin, Y.: Effects of solution chemistry on straining of colloids in porous media under unfavorable conditions. *Water Resour. Res.* (2008). doi:10.1029/2007WR006580
- Shen, C., Lazouskaya, V., Zhang, H., Wang, F., Li, B., Jin, Y., Huang, Y.: Theoretical and experimental investigation of detachment of colloids from rough collector surfaces. *Colloids Surf. A* **410**, 98–110 (2012)
- Song, L., Elimelech, M.: Calculation of particle deposition rate under unfavorable particle-surface interactions. *J. Chem. Soc. Faraday Trans.* **89**(18), 3443–3452 (1993)
- Tang, G.Q., Morrow, N.R.: Oil recovery by waterflooding—invading brine cation valency and salinity. *J. Pet. Sci. Eng.* **24**, 99–111 (1999)
- Tien, C.: *Granular Filtration of Aerosols and Hydrosols*. Butterworths Series in Chemical Engineering. Butterworths, Boston (1989)
- Torkzaban, S., Bradford, S.A., Vanderzalm, J.L., Patterson, B.M., Harris, B., Prommer, H.: Colloid release and clogging in porous media: effects of solution ionic strength and flow velocity. *J. Contam. Hydrol.* **181**, 161–171 (2015)
- Torkzaban, S., Bradford, S.A., Walker, S.L.: Resolving the coupled effects of hydrodynamics and DLVO forces on colloid attachment in porous media. *Langmuir* **23**, 9652–9660 (2007)
- Tosco, T., Bosch, J., Meckenstock, R.U., Sethi, R.: Transport of ferrihydrite nanoparticles in saturated porous media: role of ionic strength and flow rate. *Environ. Sci. Technol.* **46**, 4008–4015 (2012)

- Tripathy, A.: Hydrodynamically and chemically induced in situ kaolin particle release from porous media an experimental study. *Adv. Powder Technol.* **21**, 564–572 (2010)
- Tufenkji, N., Elimelech, M.: Correlation equation for predicting single-collector efficiency in physicochemical filtration in saturated porous media. *Environ. Sci. Technol.* **38**, 529–536 (2004)
- Tufenkji, N., Elimelech, M.: Spatial distributions of *Cryptosporidium oocysts* in porous media: evidence of dual mode deposition. *Environ. Sci. Technol.* **39**(10), 3620–3629 (2005)
- Verwey, E.J.W., Overbeek, J.T.G.: *Theory of the Stability of Lyophobic Colloids*. Elsevier, Amsterdam (1948)
- Wang, H.-Q., Lacroix, M., Massei, N., Dupont, J.-P.: Transport des particules en milieu poreux détermination des paramètres hydrodispersifs et du coefficient de dépôt. *Comptes Rendus de l'Académie des Sciences, Sciences de la Terre et des planètes* **331**, 97–104 (2000)
- Xu, S., Gao, B., Saiers, J.E.: Straining of colloidal in saturated porous media. *Water Resour. Res.* **42**, 1–10 (2006)
- Yao, K.M., Habibian, M.T., O'Melia, C.R.: Water and waste water filtration concepts and applications. *Environ. Sci. Technol.* **5**, 1105–1112 (1971)